Quantum fluctuations on top of a $\mathcal{PT}$-symmetric Bose-Einstein condensate

Xiaoling Cui ◉*

Beijing National Laboratory for Condensed Matter Physics, Institute of Physics, Chinese Academy of Sciences, Beijing 100190, China
and Songshan Lake Materials Laboratory, Dongguan, Guangdong 523808, China

We investigate the effects of quantum fluctuations in a parity-time ($\mathcal{PT}$) symmetric two-species Bose-Einstein condensate (BEC). It is found that the $\mathcal{PT}$ symmetry, though preserved by the macroscopic condensate, can be spontaneously broken by its Bogoliubov quasiparticles under quantum fluctuations. The associated $\mathcal{PT}$-breaking transitions in the Bogoliubov spectrum can be conveniently tuned by the interaction anisotropy in spin channels and the strength of $\mathcal{PT}$ potential. In the $\mathcal{PT}$-unbroken regime, the real Bogoliubov modes are generally gapped, in contrast to the gapless phonon mode in Hermitian case. Moreover, the presence of $\mathcal{PT}$ potential is found to enhance the mean-field collapse and thereby intrigue the droplet formation after incorporating the repulsive force from quantum fluctuations. These remarkable interplay effects of $\mathcal{PT}$ symmetry and interaction can be directly probed in cold atoms experiments, which shed light on related quantum phenomena in general $\mathcal{PT}$-symmetric systems.

I. INTRODUCTION

The parity-time ($\mathcal{PT}$) symmetry governs a fascinating class of non-Hermitian Hamiltonians whose energy spectra can be purely real and bounded below [1], analogous to the Hermitian ones. Nevertheless, very different from the Hermitian counterpart, their eigenstates are generally nonorthogonal and can even coalesce at exceptional points (EPs), where the $\mathcal{PT}$-breaking transition occurs and the spectra after the transition become complex [2]. The single-particle $\mathcal{PT}$-symmetric Hamiltonian and the associated breaking transitions have been successfully explored earlier in various photonic, electronic, and acoustic systems (see reviews [3,4]), and recently also in the quantum walk interferometer [5], superconducting circuit [6], nitrogen-vacancy center [7], trapped ions [8,9], and ultracold gases [10–12].

Given the intriguing single-particle property of $\mathcal{PT}$ symmetry, its interplay with interaction has become a rapidly developing research frontier in recent years [13–26]. Previous studies have focused on the interacting $\mathcal{PT}$-symmetric bosons and fermions based on mean-field analyses [13,14,17–20,26], and the phase transitions and critical phenomena near EPs [15,16,22–24]. To date, little has been said about beyond-mean-field effects with $\mathcal{PT}$ symmetry, and whether such effects can generate equally significant quantum phenomena far from EPs. Answering these questions will help to capture the very intrinsic physics in the interplay of interaction and $\mathcal{PT}$ symmetry, which will in turn shed light on related quantum phenomena in a much broader context.

In this paper, we explore the effects of quantum fluctuations on top of a $\mathcal{PT}$-symmetric two-species ($\uparrow, \downarrow$) Bose-Einstein condensate (BEC) with the non-Hermitian potential

$$V_{\mathrm{PT}} = \Omega(\sigma_x + i\gamma\sigma_z), \tag{1}$$

where $\sigma_\alpha (\alpha = x, y, z)$ are the Pauli matrices. Obviously V_{PT} commutes with the $\mathcal{PT}$ operator, with $\mathcal{P}$ flipping the spin($\uparrow \leftrightarrow \downarrow$) and $\mathcal{T}$ changing i to $-i$. In the single-particle level, the physics of V_{PT} has been well studied in literature [3–12] and the $\mathcal{PT}$ symmetry is preserved for $\gamma < 1$. Here we show that when turn on boson-boson interactions, quantum fluctuations can significantly affect the elementary excitation of the system even far from the single-particle EP. Specifically, our main findings are listed as below:

(i) The $\mathcal{PT}$ symmetry, though preserved by the condensate, can be *spontaneously broken* by the Bogoliubov quasiparticles. The $\mathcal{PT}$-breaking transition in the Bogoliubov spectrum can be conveniently tuned by the strength of V_{PT} and the interaction anisotropy in spin channels.

(ii) The quasiparticle in the $\mathcal{PT}$-unbroken regime is generally *gapped*, on contrary to the gapless mode in the Hermitian case. Moreover, the mean-field instability of a non-Hermitian system does *not necessarily* lead to imaginary excitations therein.

(iii) The presence of V_{PT} can enhance the mean-field collapse of the BEC, and thereby extend the droplet formation to a broader interaction regime than the Hermitian counterpart.

The experimental relevance of our results and the implication to a general $\mathcal{PT}$-symmetric system will also be discussed in this paper.

The rest of the paper is organized as follows. In Sec. II we present the basic model of the system, including the

*xlcui@iphy.ac.cn

single-particle physics and mean-field treatment. The followed Sec. III is contributed to the mean-field ground state. In Sec. IV, we build up a systematic theory for the Bogoliubov analysis of the non-Hermitian BEC. The resulted excitation spectrum and the droplet properties are presented, respectively, in Secs. V and VI. Finally, we discuss the experimental relevance of our results in Sec. VII and summarize the whole paper in Sec. VIII.

II. MODEL

We consider the following Hamiltonian for the interacting two-species bosons under the $\mathcal{PT}$-symmetric potential (we take $\hbar = 1$ throughout the paper)

$$
H = \int d\mathbf{r} \sum_{\alpha\beta} \left\{ \Psi_\alpha^\dagger(\mathbf{r}) \left[-\frac{\nabla^2}{2m_\alpha} \delta_{\alpha\beta} + \Omega\left(\sigma_x^{\alpha\beta} + i\gamma\sigma_z^{\alpha\beta}\right) \right] \Psi_\beta(\mathbf{r}) \right.
$$
$$
\left. + \frac{g_{\alpha\beta}}{2} \Psi_\alpha^\dagger(\mathbf{r})\Psi_\beta^\dagger(\mathbf{r})\Psi_\beta(\mathbf{r})\Psi_\alpha(\mathbf{r}) \right\}. \tag{2}
$$

Here $\alpha, \beta = \{\uparrow, \downarrow\}$, and $\{\Psi_\alpha^\dagger, \Psi_\alpha\}$ are the field operators of spin-α bosons. In order to ensure the $\mathcal{PT}$ symmetry of (2), we take the equal mass $m_\uparrow = m_\downarrow \equiv m$ and equal intraspecies coupling $g_{\uparrow\uparrow} = g_{\downarrow\downarrow} \equiv g$. In this case, the property of a homogeneous BEC is determined by three dimensionless parameters: the dissipation parameter γ, and two dimensionless combinations $\eta \equiv g_{\uparrow\downarrow}/g$ and $\tilde{\Omega} \equiv \Omega/(gn)$ (n the total density of the BEC).

A. Single-particle physics

The noninteracting part of (2) can be diagonalized as

$$
H_0 = \sum_\nu \epsilon_{\nu;\mathbf{k}} \Psi_{\nu;\mathbf{k},R}^\dagger \Psi_{\nu;\mathbf{k},L} \tag{3}
$$

where $\nu = \{+, -\}$ is the index of single-particle eigenstate with eigenenergy $\epsilon_{\nu;\mathbf{k}} = \mathbf{k}^2/(2m) + \nu\Omega\sqrt{1-\gamma^2}$; $\Psi_{\nu;\mathbf{k},R}^\dagger$ ($\Psi_{\nu;\mathbf{k},L}$) is the associated creation (annihilation) operator of the right (left) eigenstate, which satisfies the commutation relation

$$
[\Psi_{\nu';\mathbf{k}',L}, \Psi_{\nu;\mathbf{k},R}^\dagger] = \delta_{\mathbf{k}\mathbf{k}'}\delta_{\nu\nu'}. \tag{4}
$$

This relation is equivalent to the bi-orthogonality of right and left eigenstates, which is crucially important for building the theories of non-Hermitian BECs as presented later.

Since V_{PT} decouples from the kinetic term, the right/left eigenstates can be decoupled as

$$
\Psi_{\nu;\mathbf{k},R/L}^\dagger |0\rangle \equiv |\mathbf{k}\rangle |\nu\rangle_{R/L}, \tag{5}
$$

where $|0\rangle$ is the vacuum, $|\mathbf{k}\rangle$ is the plane-wave state with momentum $\mathbf{k}$, and $|\nu\rangle_{R/L}$ is the spin part of the eigenstate that is solely determined by V_{PT}. Specifically, the right and left eigenstates are defined through the Schrödinger equations:

$$
V_{PT}|\nu\rangle_R = \epsilon_\nu |\nu\rangle_R, \qquad V_{PT}^\dagger |\nu\rangle_L = \epsilon_\nu^* |\nu\rangle_L, \tag{6}
$$

with $\epsilon_\nu = \nu\Omega\sqrt{1-\gamma^2}$. In the regime $\gamma < 1$, $|\nu\rangle_{R/L}$ can be expressed as

$$
|+\rangle_R = C_{+,R}(u|\uparrow\rangle + |\downarrow\rangle); \quad |-\rangle_R = C_{-,R}(|\uparrow\rangle - u|\downarrow\rangle).
$$
$$
|+\rangle_L = C_{+,L}(|\uparrow\rangle + u|\downarrow\rangle); \quad |-\rangle_L = C_{-,L}(u|\uparrow\rangle - |\downarrow\rangle), \tag{7}
$$

with the parameter

$$
u = \sqrt{1-\gamma^2} + i\gamma. \tag{8}
$$

Here $C_{\nu,R}, C_{\nu,L}$ are all normalization factors. For the Hermitian case ($\gamma = 0$ and $u = 1$), we can see that the right and left eigenvectors become identical, i.e., $|+\rangle_R \sim |+\rangle_L$, $|-\rangle_R \sim |-\rangle_L$, and different levels are orthogonal to each other $_{R,L}\langle -|+\rangle_{R,L} = 0$. In comparison, for the non-Hermitian case ($\gamma \neq 0$ and u is complex), these relations are no longer satisfied, i.e., $|\nu\rangle_R \neq |\nu\rangle_L$ and $_R\langle -|+\rangle_R \neq 0$, $_L\langle -|+\rangle_L \neq 0$. However, given the definition of right/left eigenstates in Eq. (6), the bi-orthogonality can be satisfied as long as $\epsilon_+ \neq \epsilon_-$:

$$
_L\langle -|+\rangle_R = 0, \qquad _L\langle +|-\rangle_R = 0. \tag{9}
$$

Therefore, the normalization can be carried out between the right and left eigenvectors:

$$
_L\langle \nu|\nu\rangle_R = 1, \qquad \nu = \pm; \tag{10}
$$

which gives

$$
C_{\nu,L}^* C_{\nu,R} = \frac{1}{u + u^*}, \qquad \nu = \pm. \tag{11}
$$

Note that Eqs. (9) and (10) guarantees the commutation relation (4). In this paper, we choose a specific gauge such that the normalization factors are all real and identical:

$$
C_{\nu,R} = C_{\nu,L} = \frac{1}{\sqrt{u + u^*}}. \tag{12}
$$

In this way, when the $\mathcal{PT}$ operator acts on these eigenvectors, we have

$$
\mathcal{PT}|\nu\rangle_R = \nu u^*|\nu\rangle_R; \quad \mathcal{PT}|\nu\rangle_L = \nu u^*|+\rangle_L. \tag{13}
$$

This demonstrates that, in the $\gamma < 1$ regime, $|\nu\rangle_{R/L}$ are both the eigenstates of $\mathcal{PT}$ operator with eigenvalue νu^*. If one chooses a different gauge other than (12), the eigenvalues in (13) will be changed. However, we have checked that the gauge choice will not affect the physical quantities studied in this paper, given that (11) is satisfied.

B. Mean-field treatment of the $\mathcal{PT}$-symmetric BEC

In the mean-field framework, we can write down a general coherent ansatz for the right state of the BEC:

$$
|\Psi_0\rangle_R = \mathcal{A} \sum_n \frac{\left(\sum_\nu \sqrt{N_\nu} e^{i\theta_\nu} \Psi_{\nu;\mathbf{k}=0,R}^\dagger\right)^n}{n!} |0\rangle. \tag{14}
$$

Here N_ν and θ_ν are respectively the mean number and the phase of the condensate at level ν. In the regime $\gamma < 1$, since the single-particle state $\Psi_{\nu;\mathbf{k},R/L}^\dagger |0\rangle$ preserves the $\mathcal{PT}$ symmetry, it is natural to require the condensate (14) equally preserve such symmetry. Given Eq. (13), this requirement leads to

$$
e^{2i\theta_\nu} = \nu u^*. \tag{15}
$$

Following the same strategy, we can obtain the left state of the BEC, $|\Psi_0\rangle_L$, which shares the same form as (14) except replacing $\Psi_{\nu;\mathbf{k}=0,R}^\dagger$ by $\Psi_{\nu;\mathbf{k}=0,L}^\dagger$.

Given the commutation relation (4) and the coherent ansatz (14), we can obtain the following expectation values under the

bi-orthogonal basis:

$$
\begin{aligned}
&_L\langle\Psi_0|\Psi^\dagger_{\nu;\mathbf{k}=0,R}|\Psi_0\rangle_R = \sqrt{N_\nu}e^{-i\theta_\nu},\\
&_L\langle\Psi_0|\Psi_{\nu;\mathbf{k}=0,L}|\Psi_0\rangle_R = \sqrt{N_\nu}e^{i\theta_\nu};\\
&_L\langle\Psi_0|\Psi^\dagger_{\nu;\mathbf{k}=0,R}\Psi_{\nu';\mathbf{k}=0,L}|\Psi_0\rangle_R = \sqrt{N_\nu N_{\nu'}}e^{i(\theta_{\nu'}-\theta_\nu)};\\
&_L\langle\Psi_0|\Psi^\dagger_{\nu;\mathbf{k}=0,R}\Psi^\dagger_{\nu';\mathbf{k}=0,R}\Psi_{\nu'';\mathbf{k}=0,L}\Psi_{\nu''';\mathbf{k}=0,L}|\Psi_0\rangle_R\\
&\quad = \sqrt{N_\nu N_{\nu'} N_{\nu''} N_{\nu'''}}e^{i(\theta_{\nu''}+\theta_{\nu'''}-\theta_{\nu'}-\theta_\nu)}.
\end{aligned}
\tag{16}
$$

This shows that in the mean-field framework under the bi-orthogonal basis, one can replace the zero-momentum operators $\Psi^\dagger_{\nu;\mathbf{k}=0,R}$ and $\Psi_{\nu;\mathbf{k}=0,L}$ with their mean values:

$$
\Psi^\dagger_{\nu;\mathbf{k}=0,R} \to \sqrt{N_\nu}e^{-i\theta_\nu}, \quad \Psi_{\nu;\mathbf{k}=0,L} \to \sqrt{N_\nu}e^{i\theta_\nu}.
\tag{17}
$$

In this way, we can go on to study the mean-field ground state and examine the effects of quantum fluctuations on top of it.

Here we would like to emphasize that the mean-field treatment is only valid under the bi-orthogonal basis, but not if only use one of the basis (right or left). For instance, we cannot obtain the expectation values as the form in Eq. (16) if only under the right basis ($_R\langle...\rangle_R$) or the left basis ($_L\langle...\rangle_L$), and as a result we cannot replace the operators by their according mean-field values as in (17).

C. Interaction channels

To facilitate later discussions, we rewrite the interaction part of (2) in the following form:

$$
U = \sum_{\nu_1\nu_2\nu_3\nu_4} U_{\nu_1\nu_2;\nu_3\nu_4} \sum_{\mathbf{Qkk'}} \Psi^\dagger_{\nu_1;\mathbf{Q}-\mathbf{k},R}\Psi^\dagger_{\nu_2;\mathbf{k},R}\Psi_{\nu_3;\mathbf{k'},L}\Psi_{\nu_4;\mathbf{Q}-\mathbf{k'},L}.
\tag{18}
$$

Here $U_{\nu_1\nu_2;\nu_3\nu_4}$ is invariant under the permutation of $\nu_1 \leftrightarrow \nu_2$ or $\nu_3 \leftrightarrow \nu_4$, and thus there are totally nine different coupling channels, with five even-parity combinations $\{\nu_1\nu_2;\nu_3\nu_4\} = \{++;++\}, \{--;--\}, \{++;--\}, \{--;++\}, \{+-;+-\}$, and four odd-parity ones $\{+-;++\}, \{+-;--\}, \{++;+-\}, \{--;+-\}$. The coupling constants in these channels are:

$$
U_{++;++} = U_{--;--} = \frac{g}{V}\frac{u_-}{4}; \quad U_{++;--} = U_{--;++} = \frac{g}{V}u'_+;
$$

$$
U_{+-;+-} = \frac{g}{V}u_+;
$$

$$
U_{+-;++} = -U_{+-;--} = U_{++;+-} = -U_{--;+-} = -\frac{g}{V}u'',
\tag{19}
$$

with

$$
u_- = 4u'_- = \frac{1-2\gamma^2+\eta}{1-\gamma^2}; \quad u_+ = \frac{1-\eta\gamma^2}{1-\gamma^2};
$$

$$
u'_+ = \frac{1-\eta}{4(1-\gamma^2)}; \quad u'' = -\frac{i\gamma(1-\eta)}{2(1-\gamma^2)}.
\tag{20}
$$

Here u_-, u_+, and u'_+ are the coupling constants for even-parity channels, and u'' represents the coupling for odd-parity ones. u'' is nonzero and purely imaginary only for the non-Hermitian case with spin-independent interaction, i.e., when $\gamma \neq 0$ and $\eta \neq 1$. As shown later, the presence of these odd-parity channels will greatly affect the elementary excitation of the BEC.

III. MEAN-FIELD GROUND STATE

To determine the mean-field ground state, we examine the total mean-field energy $E_{\text{mf}} =_L \langle\Psi_0|H|\Psi_0\rangle_R$. It is found that under the phase constraint (15), E_{mf} solely depends on the parameter $x \equiv N_-/N$, where $N = N_- + N_-$ is the total number. Explicitly, the energy per particle $\epsilon_{\text{mf}} \equiv E_{\text{mf}}/N$ reads

$$
\epsilon_{\text{mf}}(x) = \Omega\sqrt{1-\gamma^2}(1-2x)
$$
$$
+ \frac{gn}{1-\gamma^2}\left(\gamma^2(\eta-1)(x^2-x) + \frac{1-2\gamma^2+\eta}{4}\right).
\tag{21}
$$

For simplicity, in this paper we will focus on the $\eta < 1$ regime, where the minimum of $\epsilon_{\text{mf}}(x)$ locates at $x = 1$, i.e., the bosons condense at the lower branch with energy

$$
\epsilon_{\text{mf}} = -\Omega\sqrt{1-\gamma^2} + \frac{gn}{1-\gamma^2}\frac{1-2\gamma^2+\eta}{4}.
\tag{22}
$$

Accordingly, we can obtain the chemical potential $\mu \equiv \partial E_{\text{mf}}/\partial N$ and further the compressibility $\chi \equiv \partial n/\partial\mu$ as

$$
\chi = \frac{2}{g}\frac{1-\gamma^2}{1-2\gamma^2+\eta}.
\tag{23}
$$

The mean-field stability against density fluctuations would require $\chi > 0$ and therefore

$$
\eta > 2\gamma^2 - 1.
\tag{24}
$$

This condition is more stringent than the Hermitian case ($\eta > -1$). In other words, a non-Hermitian BEC (with finite γ) can undergo mean-field collapse more easily than its Hermitian counterpart ($\gamma = 0$). This will be responsible for the γ-induced droplet formation as discussed later.

IV. BOGOLIUBOV ANALYSIS

Given the $\mathcal{PT}$-symmetric BEC at $\mathbf{k} = 0$ and $\nu = -$, we now study its elementary excitations due to quantum fluctuations. Following the standard Bogoliubov approach, we assume $\Psi^\dagger_{\nu;\mathbf{k},R}$ and $\Psi_{\nu;\mathbf{k},L}$ (except for $\{\nu = -, \ \mathbf{k} = 0\}$) are all small fluctuation operators and only keep in the Hamiltonian all the bilinear terms of these operators, which gives $H = N\epsilon_{\text{mf}} + H_{\text{BG}}$ with

$$
H_{\text{BG}} = \sum_{\mathbf{k}}\sum_{\nu}\left((\epsilon_{\nu;\mathbf{k}} - \mu + gnu_\nu)\Psi^\dagger_{\nu;\mathbf{k},R}\Psi_{\nu;\mathbf{k},L} + gnu'_\nu(e^{2i\theta_-}\Psi^\dagger_{\nu;\mathbf{k},R}\Psi^\dagger_{\nu;-\mathbf{k},R} + e^{-2i\theta_-}\Psi_{\nu;\mathbf{k},L}\Psi_{\nu;-\mathbf{k},L})\right)
$$
$$
+ gnu''\sum_{\mathbf{k}}\left(e^{2i\theta_-}\Psi^\dagger_{+;\mathbf{k},R}\Psi^\dagger_{-;-\mathbf{k},R} + e^{-2i\theta_-}\Psi_{+;\mathbf{k},L}\Psi_{-;-\mathbf{k},L} + 2\Psi^\dagger_{+;\mathbf{k},R}\Psi_{-;\mathbf{k},L} + 2\Psi^\dagger_{-;\mathbf{k},R}\Psi_{+;\mathbf{k},L}\right).
\tag{25}
$$

Here H_{BG} naturally inherits $\mathcal{PT}$ symmetry from the full Hamiltonian (2), since we have taken the condensate (14) as $\mathcal{PT}$ symmetric. The first line in H_{BG} is reduced from even-parity channels, and the second line from odd-parity

ones. Obviously, the effect of odd-parity channels is to couple fluctuations in different branches ($- \leftrightarrow +$), and the coupling constant u'' is purely imaginary in the presence of both non-Hermiticity and interaction anisotropy.

To facilitate the diagonalization of the bilinear Hamiltonian (25), we rewrite it as

$$H_{\mathrm{BG}} = \sum_{\mathbf{k}}' \left\{ F_{\mathbf{k}}^T \mathcal{M}(\mathbf{k}) G_{\mathbf{k}} - \sum_{\nu} (\epsilon_{\nu;\mathbf{k}} - \mu + g n u_\nu) \right\}, \quad (26)$$

where $\sum'$ implies the summation be taken over half of $\mathbf{k}$ space to avoid the double counting; the vectors are

$$F_{\mathbf{k}} = \begin{pmatrix} \Psi^\dagger_{-;\mathbf{k},R} \\ \Psi_{-;-\mathbf{k},L} \\ \Psi^\dagger_{+;\mathbf{k},R} \\ \Psi_{+;-\mathbf{k},L} \end{pmatrix}, \quad G_{\mathbf{k}} = \begin{pmatrix} \Psi_{-;\mathbf{k},L} \\ \Psi^\dagger_{-;-\mathbf{k},R} \\ \Psi_{+;\mathbf{k},L} \\ \Psi^\dagger_{+;-\mathbf{k},R} \end{pmatrix}; \quad (27)$$

and the matrix $\mathcal{M}$ is

$$\mathcal{M}(\mathbf{k}) = \begin{pmatrix} \epsilon_{-;\mathbf{k}} - \mu + g n u_- & 2 g n u'_- e^{2i\theta_-} & 2 g n u'' & g n u'' e^{2i\theta_-} \\ 2 g n u'_- e^{-2i\theta_-} & \epsilon_{-;\mathbf{k}} - \mu + g n u_- & g n u'' e^{-2i\theta_-} & 2 g n u'' \\ 2 g n u'' & g n u'' e^{2i\theta_-} & \epsilon_{+;\mathbf{k}} - \mu + g n u_+ & 2 g n u'_+ e^{2i\theta_-} \\ g n u'' e^{-2i\theta_-} & 2 g n u'' & 2 g n u'_+ e^{-2i\theta_-} & \epsilon_{+;\mathbf{k}} - \mu + g n u_+ \end{pmatrix}. \quad (28)$$

We aim to diagonalize H_{BG} as the following form:

$$H_{\mathrm{BG}} = \sum_{\mathbf{k}}' \tilde{F}_{\mathbf{k}}^T \begin{pmatrix} E_{1\mathbf{k}} & & & \\ & E_{2\mathbf{k}} & & \\ & & E_{3\mathbf{k}} & \\ & & & E_{4\mathbf{k}} \end{pmatrix} \tilde{G}_{\mathbf{k}} + \mathrm{const}, \quad (29)$$

where $E_{i\mathbf{k}}$ are the four eigenmodes for Bogoliubov quasiparticles, and the two eigenvectors are

$$\tilde{F}_{\mathbf{k}} = \begin{pmatrix} \alpha^\dagger_{1,\mathbf{k},R} \\ \alpha_{2,\mathbf{k},L} \\ \alpha^\dagger_{3,\mathbf{k},R} \\ \alpha_{4,\mathbf{k},L} \end{pmatrix}, \quad \tilde{G}_{\mathbf{k}} = \begin{pmatrix} \alpha_{1,\mathbf{k},L} \\ \alpha^\dagger_{2,\mathbf{k},R} \\ \alpha_{3,\mathbf{k},L} \\ \alpha^\dagger_{4,\mathbf{k},R} \end{pmatrix}. \quad (30)$$

The eigenoperators are required to satisfy the commutation relation

$$[\alpha_{i,\mathbf{k},L}, \alpha^\dagger_{j,\mathbf{k}',R}] = \delta_{ij}\delta_{\mathbf{kk}'}, \quad i, j = 1, 2, 3, 4. \quad (31)$$

To find out eigenspectra $E_{i\mathbf{k}}$ as well as the relation between $\tilde{F}_{\mathbf{k}}, \tilde{G}_{\mathbf{k}}$ and $F_{\mathbf{k}}, G_{\mathbf{k}}$, we start from the equation of motions (EoM) of these vectors. Based on the Heisenberg equation for non-Hermitian system (see derivation in Appendix), we can write down the EoM of $G_{\mathbf{k}}$ and $\tilde{G}_{\mathbf{k}}$:

$$i\frac{\partial}{\partial t} G_{\mathbf{k}} = \begin{pmatrix} 1 & & & \\ & -1 & & \\ & & 1 & \\ & & & -1 \end{pmatrix} \mathcal{M}(\mathbf{k}) G_{\mathbf{k}};$$

$$i\frac{\partial}{\partial t} \tilde{G}_{\mathbf{k}} = \begin{pmatrix} E_{1\mathbf{k}} & & & \\ & -E_{2\mathbf{k}} & & \\ & & E_{3\mathbf{k}} & \\ & & & -E_{4\mathbf{k}} \end{pmatrix} \tilde{G}_{\mathbf{k}}. \quad (32)$$

This implies that by diagonalizing the matrix diag $(1, -1, 1, -1)\mathcal{M}(\mathbf{k})$, we can obtain the four Bogoliubov modes from its eigenenergies. Explicitly, by introducing a

transformation matrix $\mathcal{A}$ in $G_{\mathbf{k}} = \mathcal{A}\tilde{G}_{\mathbf{k}}$, we have

$$\mathcal{A}^{-1} \left[\begin{pmatrix} 1 & & & \\ & -1 & & \\ & & 1 & \\ & & & -1 \end{pmatrix} \mathcal{M}(\mathbf{k}) \right] \mathcal{A}$$

$$= \begin{pmatrix} E_{1\mathbf{k}} & & & \\ & -E_{2\mathbf{k}} & & \\ & & E_{3\mathbf{k}} & \\ & & & -E_{4\mathbf{k}} \end{pmatrix}. \quad (33)$$

Similarly, we can write down the EoM for $F_{\mathbf{k}}$ and $\tilde{F}_{\mathbf{k}}$, and by introducing a transformation matrix $\mathcal{B}$ in $F_{\mathbf{k}}^T = \tilde{F}_{\mathbf{k}}^T \mathcal{B}$, we have

$$\mathcal{B} \left[\mathcal{M}(\mathbf{k}) \begin{pmatrix} -1 & & & \\ & 1 & & \\ & & -1 & \\ & & & 1 \end{pmatrix} \right] \mathcal{B}^{-1}$$

$$= \begin{pmatrix} -E_{1\mathbf{k}} & & & \\ & E_{2\mathbf{k}} & & \\ & & -E_{3\mathbf{k}} & \\ & & & E_{4\mathbf{k}} \end{pmatrix}. \quad (34)$$

Therefore, the Bogoliubov modes can also be obtained by diagonalizing the matrix $\mathcal{M}(\mathbf{k})\mathrm{diag}(-1, 1, -1, 1)$.

The two diagonalization schemes, i.e., one is based on (33) and the other is based on (34), produce the same solution of $E_{i\mathbf{k}}$, which satisfy

$$E_{\mathbf{k}} = \sqrt{\frac{-b_{\mathbf{k}} \pm \sqrt{b_{\mathbf{k}}^2 - 4c_{\mathbf{k}}}}{2}}, \quad (35)$$

with

$$b_{\mathbf{k}} = -(\epsilon_{-;\mathbf{k}} - \mu + g n u_-)^2 - (\epsilon_{+;\mathbf{k}} - \mu + g n u_+)^2 - (gn)^2(6u''^2 - 4u_+'^2 - 4u_-'^2);$$

$$c_{\mathbf{k}} = [(\epsilon_{-;\mathbf{k}} - \mu + g n u_-)^2 - (2g n u'_-)^2][(\epsilon_{+;\mathbf{k}} - \mu + g n u_+)^2 - (2g n u'_+)^2]$$

$$+ (gnu'')^2[9(gnu'')^2 - 40(gn)^2u'_-u'_+$$
$$- 10(\epsilon_{-;\mathbf{k}} - \mu + gnu_-)(\epsilon_{+;\mathbf{k}} - \mu + gnu_+)$$
$$+ 16gnu'_+(\epsilon_{-;\mathbf{k}} - \mu + gnu_-)$$
$$+ 16gnu'_-(\epsilon_{+;\mathbf{k}} - \mu + gnu_+)]. \quad (36)$$

The four eigenmodes in (35) fall into two identical pairs, and we choose $E_{1\mathbf{k}} = E_{2\mathbf{k}}$ and $E_{3\mathbf{k}} = E_{4\mathbf{k}}$. This is also a natural choice since in noninteracting limit, $\mathcal{M}(\mathbf{k})$ can exactly reduce to the diagonal matrix diag$(E_{1\mathbf{k}}, E_{2\mathbf{k}}, E_{3\mathbf{k}}, E_{4\mathbf{k}})$ with $E_{1\mathbf{k}} = E_{2\mathbf{k}}$ and $E_{3\mathbf{k}} = E_{4\mathbf{k}}$.

In fact, based on the commutation relations (4) and (31), we can find out the relation between the two transformation matrices:

$$\mathcal{A} \begin{pmatrix} 1 & & & \\ & -1 & & \\ & & 1 & \\ & & & -1 \end{pmatrix} \mathcal{B} = \begin{pmatrix} 1 & & & \\ & -1 & & \\ & & 1 & \\ & & & -1 \end{pmatrix}, \quad (37)$$

and then one can prove straightforwardly that $\mathcal{B}\mathcal{M}(\mathbf{k})\mathcal{A} = $ diag$(E_{1\mathbf{k}}, E_{2\mathbf{k}}, E_{3\mathbf{k}}, E_{4\mathbf{k}})$. It follows that the first term in Eq. (26) is equal to the first term in Eq. (29). Therefore the constant terms in (26) and (29) are also identical. Now we can rewrite Eq. (29) as

$$H_{\mathrm{BG}} = \sum_{\mathbf{k}}' \sum_{i=1}^{4} E_{i\mathbf{k}} \alpha_{i,\mathbf{k},R}^{\dagger} \alpha_{i,\mathbf{k},L} + \frac{1}{2} \sum_{\mathbf{k}} \left\{ E_{1\mathbf{k}} + E_{3\mathbf{k}} \right.$$
$$\left. - \sum_{\nu}(\epsilon_{\nu;\mathbf{k}} - \mu + gnu_\nu) \right\}, \quad (38)$$

Further incorporating the regularization of bare couplings g and g_{12} from the mean-field interaction energy (22), we can obtain the Lee-Huang-Yang (LHY) energy as:

$$E_{\mathrm{LHY}} = \frac{1}{2} \sum_{\mathbf{k}} \left\{ E_{1\mathbf{k}} + E_{3\mathbf{k}} - \sum_{\nu}(\epsilon_{\nu;\mathbf{k}} - \mu + gnu_\nu) \right.$$
$$\left. + \frac{1 - 2\gamma^2 + \eta^2}{2(1 - \gamma^2)} \frac{m(gn)^2}{\mathbf{k}^2} \right\}. \quad (39)$$

We have checked that the summation in above equation converges at large $\mathbf{k}$ and the ultraviolet divergence can be avoided.

V. EXCITATION SPECTRUM

In this section, we present the result of Bogoliubov excitation spectrum for the $\mathcal{PT}$-symmetric BEC. Since $E_{1\mathbf{k}} = E_{2\mathbf{k}}$ and $E_{3\mathbf{k}} = E_{4\mathbf{k}}$, we will only show the results of $E_{1\mathbf{k}}$ and $E_{3\mathbf{k}}$.

To highlight the effect of non-Hermiticity to Bogoliubov excitations, we first go through the Hermitian case ($\gamma = 0$). In this case, all odd-parity terms in (25) are absent ($u'' = 0$) and the fluctuations in $+$ and $-$ branches are well decoupled. This leads to a gapless spectrum $E_{1\mathbf{k}} = \sqrt{(k^2/2m)^2 + 2\mu_- k^2/(2m)}$ and a gapped one $E_{3\mathbf{k}} = \sqrt{(k^2/2m + 2\Omega)^2 + 2\mu_+(k^2/2m + 2\Omega)}$, with $\mu_\pm = gn(1 \mp \eta)/2$. Clearly, in the mean-field collapse regime with $\eta < -1$, the lower spectrum $E_{1\mathbf{k}}$ becomes purely imaginary near $\mathbf{k} \sim 0$, signifying the dynamical instability. In addition, we note that under certain condition the two spectra become degenerate,
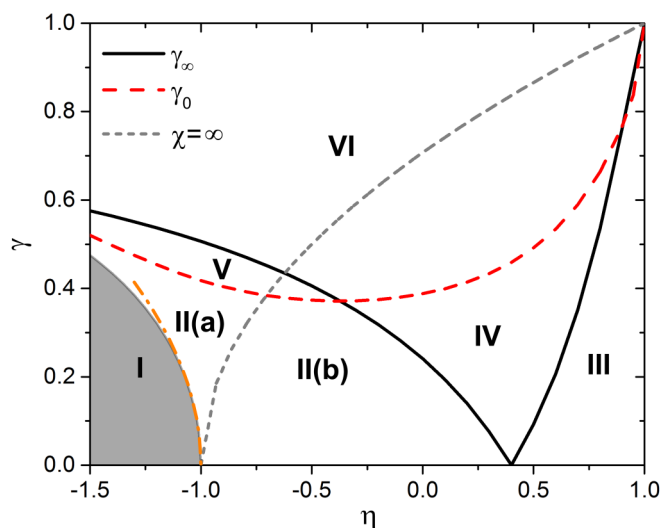

FIG. 1. Diagrams in (γ, η) plane that exhibit different excitation properties. Here $\tilde{\Omega} = 0.2$. "I" marks the region where the excitation spectrum at low $\mathbf{k}$ is purely imaginary. "II" is the region where all spectra are real and gapped. The gray dashed line sets the mean-field collapse boundary, which further divides II into II(a) ($\chi < 0$) and II(b) ($\chi > 0$). $\mathcal{PT}$-breaking transition of Bogoliubov modes occurs in regions III, IV, and V, where the spectra become complex either within intermediate $|\mathbf{k}| \equiv k(\mathrm{III})$, or at large $k(\mathrm{IV})$, or low $k(\mathrm{V})$. In VI, the complex spectra occur for all $\mathbf{k}$. These regions are separated by the curves of γ_0 and γ_∞, which, respectively, are the values of γ when the spectra becomes complex at $k = 0$ and $k \to \infty$.

i.e., $E_{1\mathbf{k}_0} = E_{3\mathbf{k}_0}$ at:

$$|\mathbf{k}_0| = \sqrt{2m\Omega((\eta - 2\tilde{\Omega})^{-1} - 1)}, \quad \text{if } 0 < \eta - 2\tilde{\Omega} < 1. \quad (40)$$

The according plot is given in Fig. 2(a). This feature will lead to interesting excitation property when turn on γ.

In the presence of non-Hermiticity ($\gamma \neq 0$), the interbranch fluctuations give two important impacts on the Bogoliubov modes, namely, the spontaneous $\mathcal{PT}$-symmetry breaking and the gapped excitation, as detailed below.

A. Spontaneous $\mathcal{PT}$-symmetry breaking

Although $\mathcal{PT}$ symmetry is preserved by H, H_{BG}, and the condensate $|\Psi_0\rangle_{R,L}$, it can be spontaneously broken by the Bogoliubov quasiparticles, as manifested by the appearance of complex $E_{i\mathbf{k}}$. The $\mathcal{PT}$-broken region in $\mathbf{k}$ space sensitively depends on parameters $\tilde{\Omega}$, η, and γ. In Fig. 1, we have divided (γ, η) plane into different regions (I-VI) according to different $\mathcal{PT}$-breaking properties in the Bogoliubov spectra for a fixed $\tilde{\Omega} = 0.2$. The complex spectra occur in regions III-VI.

Let us start from region III with a small γ and $2\tilde{\Omega} < \eta < 1$ [satisfying the condition in (40)]. In this case, a finite γ will lead to the $\mathcal{PT}$ breaking of excitation spectra near $\mathbf{k}_0$. As shown in Figs. 2(b1) and 2(b2), for $\gamma = 0.15$, $E_{1\mathbf{k}}$ and $E_{3\mathbf{k}}$ are complex and conjugate to each other within a finite window $|\mathbf{k}| \equiv k \in (k_1, k_2)$. Thus, as increasing k from zero, the $\mathcal{PT}$ symmetry breaks at k_1 and then revives at k_2. The critical

boundaries k_1, k_2, which are determined by the solutions to $b_{\mathbf{k}}^2 - 4c_{\mathbf{k}} = 0$, sensitively depend on γ, see Fig. 2(c). At

small γ, we find that $k_{1,2}$ deviate from k_0 by a small shift $\delta \equiv |k - k_0|$, with

$$\frac{\delta}{k_0} = \gamma \frac{(1-\eta)\sqrt{16\tilde{k}_0^4 + 2\tilde{k}_0^2(4 + 3\eta + 10\tilde{\Omega}) + (1+\eta)(2\tilde{\Omega} - \eta + 1)}}{4\tilde{k}_0^2(\eta - 2\tilde{\Omega})} + o(\gamma^2). \tag{41}$$

Here $\tilde{k}_0 = k_0/\sqrt{2mgn}$. As shown by the dashed lines in Fig. 2(c), the dominant linear shifts based on above equation fit well to $k_{1,2}$ in small γ limit.

Continuously increasing γ, k_2, and k_1 respectively flow to ∞ and 0 at γ_∞ and γ_0. This tells that the spectra at large k become complex if $\gamma > \gamma_\infty$, and the complex spectra extend to $k = 0$ if $\gamma > \gamma_0$. Numerically, γ_0 is determined by satisfying $b_{k=0}^2 = 4c_{k=0}$. To find out γ_∞ accurately, we expand the function $F_{\mathbf{k}} \equiv b_{\mathbf{k}}^2 - 4c_{\mathbf{k}}$ at large $k \to \infty$ and only keep its leading order $\sim k^4$. Then γ_∞ is determined by the coefficient

of this leading term crossing zero, which gives the equation:

$$\eta^2 + \frac{4\gamma_\infty^2(\eta-1)}{1-\gamma_\infty^2} + 4\tilde{\Omega}^2(1 - \gamma_\infty^2) = \frac{4\tilde{\Omega}(\eta + \gamma_\infty^2(\eta-2))}{\sqrt{1-\gamma_\infty^2}}. \tag{42}$$

We can see that the above equation support a solution $\gamma_\infty = 0$ at $\eta = 2\tilde{\Omega}$. This is also consistent with Eq. (40), which tells that the degenerate point k_0 goes to ∞ in the Hermitian case if $\eta = 2\tilde{\Omega}$.

In Fig. 1, γ_0 and γ_∞ are plotted as functions of η, and accordingly regions III-IV are separated. Specifically, the $\mathcal{PT}$ breaking of Bogoliubov modes occur within a finite k window in III (with $\gamma < \gamma_0, \gamma_\infty$), at large k in IV ($\gamma_\infty < \gamma < \gamma_0$), at small k in V ($\gamma_0 < \gamma < \gamma_\infty$), and extend the whole k space in VI ($\gamma > \gamma_0, \gamma_\infty$). The typical spectra in regions IV and V are given in Figs. 2(d) and 2(e). Therefore, the $\mathcal{PT}$-breaking transition takes place twice in III, once in IV and V, and no transition in VI. This shows that the $\mathcal{PT}$ symmetry of Bogoliubov modes can be conveniently tuned by γ and η.

B. Gapped excitation

In the $\mathcal{PT}$-unbroken region, such as II in Fig. 1, the real Bogoliubov modes are gapped, instead of gapless as in Hermitian case. For $\gamma \ll 1$, we find that the excitation gap scales linearly with γ:

$$\frac{E_{1\mathbf{k}=0}}{gn} = \gamma \frac{1-\eta}{2}\sqrt{\frac{1+\eta}{2\tilde{\Omega}}}. \tag{43}$$

Such a gapped spectrum is in distinct contrast to the gapless mode in the Hermition BEC. It is closely related to the presence of imaginary odd-parity terms in (25), such as $\Psi_{+;\mathbf{k},R}^\dagger \Psi_{-;\mathbf{k},L}$, which directly couple the condensed atoms at "$-$" branch with higher "$+$" branch crossing a finite energy gap. Such coupling takes no effect for a $\mathcal{PT}$ symmetric BEC in the mean-field level but plays an important role in its quantum fluctuations. Because such imaginary coupling only exists for $\gamma \neq 0$ and $\eta \neq 1$, the quasiparticle is gapped in the same regime [see (43)]. In Fig. 3, we extract the energy gap as a function of γ for two typical η, which fit well to (43) in small γ regime.

Interestingly, the gapped excitation appears not only in the mean-field stable regime [region II(b)], but can also extend to the collapse regime [II(a)]. This is in distinct contrast to the Hermitian case where the low-k spectrum is purely imaginary in the mean-field collapse side. It is to say, the mean-field instability in non-Hermitian system does not necessarily lead to imaginary excitations. In fact, for a given $\eta < -1$, the excitation spectra can turn from purely imaginary to purely
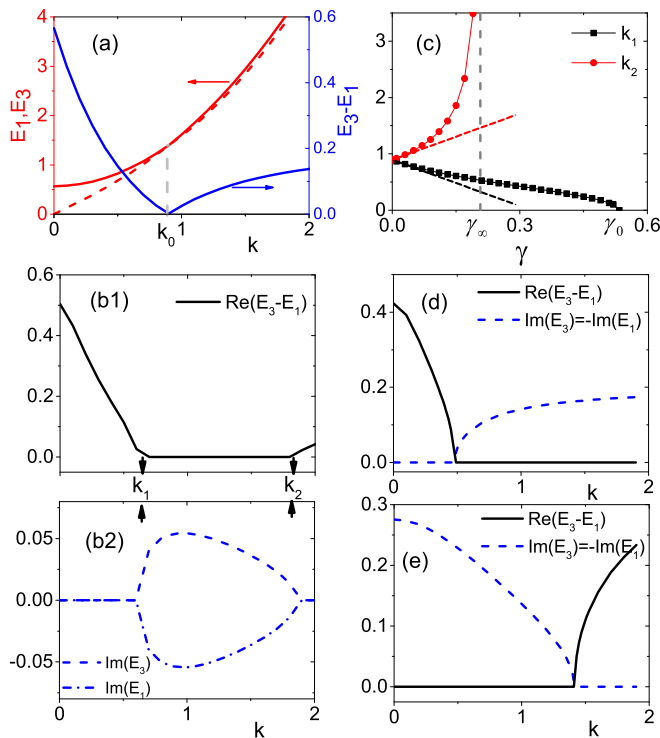

FIG. 2. Spontaneous $\mathcal{PT}$-symmetry breaking in the Bogoliubov spectra. Here $\tilde{\Omega} = 0.2$, and $\eta = 0.6$ for (a)–(c). (a) Two real spectra for Hermitian case ($\gamma = 0$), which merge at $k \equiv |\mathbf{k}| = k_0$ [see Eq. (40)]. [(b1,b2)] Real and imaginary parts of the spectra at $\gamma = 0.15$ (staying in region III), which shows $\mathcal{PT}$-symmetry breaking for $k \in (k_1, k_2)$. (c) $\mathcal{PT}$-breaking boundaries k_1 and k_2 as functions of γ. Dashed lines show linear fits for small γ [see Eq. (41)]. k_1 touches zero at γ_0 and k_2 goes to ∞ at γ_∞. [(d),(e)] Excitation spectra for $\eta = 0.4$, $\gamma = 0.3$ (region IV) and for $\eta = -0.8$, $\gamma = 0.45$ (region V), where the $\mathcal{PT}$ breaking occurs, respectively, at high k and low k. Here the momentum and energy units are, respectively, $\sqrt{2mgn}$ and gn.
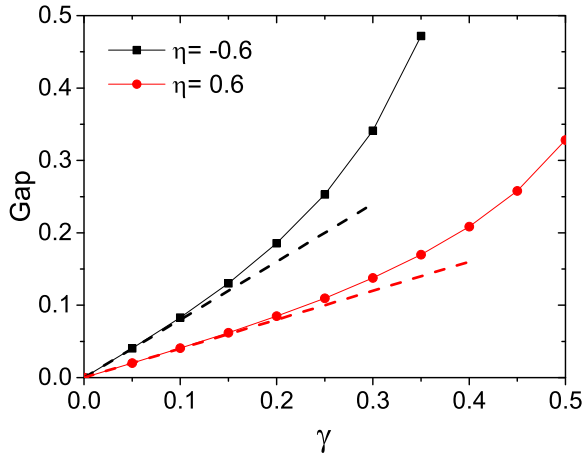
FIG. 3. Excitation gap as a function of γ for $\eta = -0.6$ and 0.6. Dashed lines show the respective function fit according to Eq. (43). Here $\tilde{\Omega} = 0.2$. The energy unit is gn.

FIG. 4. Contour plot of f-function [see Eq. (46)] in the (γ, η) plane with $\tilde{\Omega} = 0.2$.

real as increasing γ across a critical γ_c, at which point the spectrum is gapless $E_{1,\mathbf{k}=0} = 0$. In Fig. 1, we mark the $\gamma < \gamma_c$ region ("I") as shaded area, where the low-energy excitation spectra are purely imaginary.

Numerically, γ_c is determined by $c_{\mathbf{k}=0} = 0$, and thus

$$\frac{9\gamma_c^2(1-\eta)^2}{4} = -\left(1 + \eta - 2\gamma_c^2\right)\left[2\tilde{\Omega}\left(1 - \gamma_c^2\right)^{3/2}\right.$$
$$\left. + (1-\eta)\left(1 + \gamma_c^2\right)\right]. \quad (44)$$

We can see that $\gamma_c = 0$ when $\eta = -1$, reproducing the mean-field collapse point for the Hermitian case. When η slightly deviates from -1, we have

$$\gamma_c = \sqrt{-(1+\eta)\frac{2\tilde{\Omega}+2}{5-4\tilde{\Omega}}}, \quad (45)$$

which shows that γ_c scales as the square root of the deviation, as displayed by the orange dash-dot line in Fig. 1.

VI. γ-INDUCED DROPLET

The fact that the non-Hermiticity γ enhances the mean-field collapse [as inferred by Eq. (24)] renders the formation of a self-bound droplet after incorporating the LHY correction from quantum fluctuations. In general, Eq. (39) gives $\mathcal{E}_{\mathrm{LHY}} \equiv E_{\mathrm{LHY}}/V$ as:

$$\mathcal{E}_{\mathrm{LHY}} = (2m)^{3/2}(gn)^{5/2} f(\gamma, \eta, \tilde{\Omega}), \quad (46)$$

where f is a dimensionless functional. In Fig. 4, we show the contour plot of f in (γ, η) plane given a fixed $\tilde{\Omega} = 0.2$. We can see that f, or equivalently $\mathcal{E}_{\mathrm{LHY}}$, decreases continuously as γ increases and can even turn negative. Fortunately, in region II(a), which is the mean-field collapse regime with real and gapped spectra, the LHY force is always repulsive. A self-bound droplet state can then be supported in this region with zero pressure, i.e., $\partial(E/N)/\partial n = 0$, with $E = E_{\mathrm{mf}} + E_{\mathrm{LHY}}$. This gives the equilibrium density of the droplet as

$$n_{\mathrm{eq}} = \left(\frac{1 - 2\gamma^2 + \eta}{1 - \gamma^2}\right)^2 \frac{1}{36(2mg)^3 f^2(\gamma, \eta, \tilde{\Omega})}. \quad (47)$$
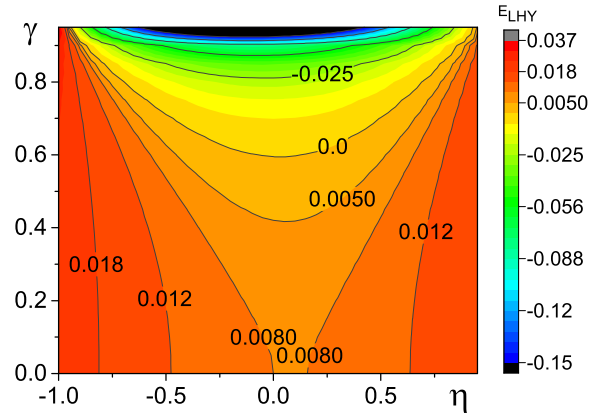
At small particle number N, the quantum pressure becomes important and drives the droplet to gas transition. To estimate the critical number N_c at the transition, we take the similar strategy as in Ref. [27] and write down the extended Gross-Pitaevskii (GP) equation as

$$i\partial_t \Psi(\mathbf{r}) = \left(-\frac{1}{2m}\nabla_{\mathbf{r}}^2 + \frac{1 - 2\gamma^2 + \eta}{2(1-\gamma^2)}g|\Psi|^2 + \frac{\partial\mathcal{E}_{\mathrm{LHY}}}{\partial n}\right)\Psi(\mathbf{r}), \quad (48)$$

where $\Psi(\mathbf{r})$ is the wave function of the BEC and the particle number is determined by $N = \int d^3\mathbf{r}|\Psi(\mathbf{r})|^2$. By rescaling $\mathbf{r}$, Ψ, t through

$$\mathbf{r} = \tilde{\mathbf{r}}\xi, \quad \Psi = \tilde{\Psi}\sqrt{n_{\mathrm{eq}}}, \quad t = \tilde{t}m\xi^2, \quad (49)$$

with

$$\xi = \sqrt{\frac{6(1-\gamma^2)}{mgn_{\mathrm{eq}}|1 - 2\gamma^2 + \eta|}}, \quad (50)$$

we can reduce the GP equation to

$$i\partial_{\tilde{t}}\tilde{\Psi}(\tilde{\mathbf{r}}) = \left(-\tfrac{1}{2}\nabla_{\tilde{\mathbf{r}}}^2 - 3|\tilde{\Psi}|^2 + \tfrac{5}{2}|\tilde{\Psi}|^3\right)\tilde{\Psi}(\tilde{\mathbf{r}}). \quad (51)$$

It is found that Eq. (51) shares the same structure as the reduced GP equation in Hermitian case [27], which leads to the rescaled critical number $\tilde{N}_c \equiv \int d^3\tilde{\mathbf{r}}|\tilde{\Psi}|^2 = 18.65$ at the vanishing of droplet solution (droplet-gas transition). Given the scaling relation in (49), we can obtain the critical $N_c = n_{\mathrm{eq}}\xi^3\tilde{N}_c$ in our system as

$$N_c = 2\sqrt{2}f\tilde{N}_c\left(\frac{6(1-\gamma^2)}{|1 - 2\gamma^2 + \eta|}\right)^{5/2}. \quad (52)$$

We can see that both n_{eq} and N_c can be conveniently tuned by γ and η.

VII. EXPERIMENTAL RELEVANCE

A $\mathcal{PT}$-symmetric two-species BEC can be realized using two hyperfine states of ^{87}Rb bosons, $|\uparrow\rangle = |F = 1, m_F = 1\rangle$ and $|\downarrow\rangle = |F = 2, m_F = -1\rangle$. The intraspecies scattering lengths are $a_{\uparrow\uparrow} = 95a_B$, $a_{\downarrow\downarrow} = 100a_B$, which have very small relative asymmetry $|a_{\uparrow\uparrow} - a_{\downarrow\downarrow}|/(a_{\uparrow\uparrow} + a_{\downarrow\downarrow}) \sim 2.5\%$. Such a small asymmetry is expected to take little effect as long

as it is much smaller than $\tilde{\Omega}$, γ. The interspecies coupling is highly tunable via Feshbach resonance around $B_0 = 9.1$G [28–30].

For the $\mathcal{PT}$-symmetric potential (1), the σ_x term can be implemented through the two-photon microwave and rf transition [31], and $i\sigma_z$ can be realized using the laser-induced state-selective dissipation up to a constant loss term $i\Omega\gamma$ [10–12]. For realistic atomic system with such constant loss, the overall number of the system decays with time. However, the physics governed by the effective non-Hermitian Hamiltonian can still be probed under the postselection scheme, as have been successfully explored in the noninteracting atomic gases [10,12]. The validity of the effective non-Hermitian Hamiltonian requires a short-time dynamics within timescale $t \ll 1/(\Omega\gamma)$, where the impact of quantum jump can be neglected. As here we consider the weak coupling regime with $na^3 \ll 1$, which is a natural extension of and can be smoothly connected to the noninteracting regime, we do not expect the validity of the effective non-Hermitian Hamiltonian would alter too much. Moreover, it should be noted that the existing experiments on quantum droplet have exactly made use of the atom loss to observe the droplet-gas transition [32–36]. We thus expect that the γ-induced droplet can be directly probed in realistic experiments.

The property of excitation spectrum can be explored by the Bragg spectroscopy as implemented previously in various cold atoms systems [37–40]. Since such spectroscopy detects the linear response of the system to external perturbations, we expect it can directly probe the excitation spectrum of non-Hermitian system as predicted in this work. Our results, which are directly relevant to atomic gases confined in a uniform trap [41–45], can also be utilized for the trapped system under local density approximation, as successfully implemented in previous experiments [37,38,40].

VIII. SUMMARY AND DISCUSSION

In summary, we have revealed the ground state and excitation properties of a $\mathcal{PT}$-symmetric BEC, including the spontaneous $\mathcal{PT}$ breaking and gapped spectrum for Bogoliubov quasiparticles, and the enhanced mean-field collapse and the facilitated droplet formation. These results show that the quantum fluctuations on top of a $\mathcal{PT}$-symmetric BEC can lead to important and visible collective phenomena even far from the single-particle EPs, thus demonstrating the significant interplay of interaction and non-Hermiticity in bosonic system.

Finally, we point out that the intriguing excitation properties revealed in this paper can be traced back to the fundamental character of non-Hermitian systems, i.e., the nonorthogonality of eigenstates. Such nonorthogonality character covers both the single-particle states and the elementary

quasiparticles. This is why the $\mathcal{PT}$-symmetry breaking can also occur in the latter. We thus expect the phenomena revealed here are not limited to the specific $\mathcal{PT}$ potential considered in this paper, but applicable to a broad class of non-Hermitian systems with $\mathcal{PT}$ symmetry. Indeed, a recent paper has pointed out the spontaneous $\mathcal{PT}$ breaking of elementary excitations on top of a fermion superfluid [25]. These $\mathcal{PT}$-breaking phenomena are generally associated with the collective many-body EP and may lead to giant fluctuation effect [22,23]. In future, it is worth to explore the impact of collective EPs in the quantum and thermal depletions, as well as the property of BEC in other parameter regime (γ, η, $\tilde{\Omega}$) beyond the scope of this paper.

APPENDIX: HEISENBERG EQUATION FOR NON-HERMITIAN SYSTEM

We first derive the Heisenberg equation for non-Hermitian system under the bi-orthogonal basis. Given the definition of right and left states, at time t they evolve as

$$|\phi_R(t)\rangle = e^{-iHt}|\phi_R(0)\rangle, \tag{A1}$$

$$|\phi_L(t)\rangle = e^{-iH^{\dagger}t}|\phi_L(0)\rangle, \tag{A2}$$

here $|\phi_R(0)\rangle$ ($|\phi_L(0)\rangle$) is the initial right (left) state at $t = 0$. Define the time-dependent expectation value of operator $\hat{A}$ as

$$\langle\hat{A}\rangle_t \equiv \langle\phi_L(t)|\hat{A}|\phi_R(t)\rangle, \tag{A3}$$

we then have

$$\langle\hat{A}\rangle_t = \langle\phi_L(0)|e^{iHt}\hat{A}e^{-iHt}|\phi_R(0)\rangle, \tag{A4}$$

and thus the Heisenberg equation can be written as

$$i\frac{\partial}{\partial t}\langle\hat{A}\rangle_t = \langle[\hat{A}, H]\rangle_t. \tag{A5}$$

We can see that the form of Heisenberg equation (A5) is identical to the Hermitian case. Nevertheless, it has a remarkable consequence for the non-Hermitian case, i.e., $\langle\hat{A}^{\dagger}\rangle_t \neq \langle\hat{A}\rangle_t^*$, which is very different from the Hermitian case. Similar relation for the time-dependent non-Hermitian operators has been given in Ref. [46].

[1] C. M. Bender and S. Boettcher, Real Spectra in Non-Hermitian Hamiltonians Having $\mathcal{PT}$ Symmetry, Phys. Rev. Lett. **80**, 5243 (1998).

[2] N. Moiseyev, *Non-Hermitian Quantum Mechanics* (Cambridge University Press, Cambridge, 2011).

[3] V. V. Konotop, J. Yang, and D. A. Zezyulin, Nonlinear waves in $\mathcal{PT}$-symmetric systems, Rev. Mod. Phys. **88**, 035002 (2016).

[4] R. El-Ganainy, K. G. Makris, M. Khajavikhan, Z. H. Musslimani, S. Rotter, and D. N. Christodoulides, Non-Hermitian physics and PT symmetry, Nat. Phys. **14**, 11 (2018).

[5] L. Xiao, X. Zhan, Z. H. Bian, K. K. Wang, X. Zhang, X. P. Wang, J. Li, K. Mochizuki, D. Kim, N. Kawakami, W. Yi, H. Obuse, B. C. Sanders, and P. Xue, Observation of topological edge states in parity–time-symmetric quantum walks, Nat. Phys. **13**, 1117 (2017).

[6] M. Naghiloo, M. Abbasi, Y. N. Joglekar, and K. W. Murch, Quantum state tomography across the exceptional point in a single dissipative qubit, Nat. Phys. **15**, 1232 (2019).

[7] Y. Wu, W. Liu, J. Geng, X. Song, X. Ye, C.-K. Duan, X. Rong, and J. Du, Observation of parity-time symmetry breaking in a single-spin system, Science **364**, 878 (2019).

[8] L. Ding, K. Shi, Q. Zhang, D. Shen, X. Zhang, and W. Zhang, Experimental Determination of $\mathcal{PT}$-Symmetric Exceptional Points in a Single Trapped Ion, Phys. Rev. Lett. **126**, 083604 (2021).

[9] W.-C. Wang, Y.-L. Zhou, H.-L. Zhang, J. Zhang, M.-C. Zhang, Y. Xie, C.-W. Wu, T. Chen, B.-Q. Ou, W. Wu, H. Jing, and P.-X. Chen, Observation of $\mathcal{PT}$-symmetric quantum coherence in a single-ion system, Phys. Rev. A **103**, L020201 (2021).

[10] J. Li, A. K. Harter, J. Liu, L. de Melo, Y. N. Joglekar, and L. Luo, Observation of parity-time symmetry breaking transitions in a dissipative Floquet system of ultracold atoms, Nat. Commun. **10**, 855 (2019).

[11] S. Lapp, J. Ang'ong'a, F. Alex An, and B. Gadway, Engineering tunable local loss in a synthetic lattice of momentum states, New J. Phys. **21**, 045006 (2019).

[12] Z. Ren, D. Liu, E. Zhao, C. He, K. K. Pak, J. Li, and G.-B. Jo, Chiral control of quantum states in non-Hermitian spin-orbit-coupled fermions, arXiv:2106.04874.

[13] H. Cartarius and G. Wunner, Model of a $\mathcal{PT}$-symmetric Bose-Einstein condensate in a δ-function double-well potential, Phys. Rev. A **86**, 013612 (2012).

[14] D. A. Zezyulin and V. V. Konotop, Nonlinear currents in a ring-shaped waveguide with balanced gain and dissipation, Phys. Rev. A **94**, 043853 (2016).

[15] V. Tripathi, A. Galda, H. Barman, and V. M. Vinokur, Parity-time symmetry-breaking mechanism of dynamic Mott transitions in dissipative systems, Phys. Rev. B **94**, 041104(R) (2016).

[16] Y. Ashida, S. Furukawa, and M. Ueda, Parity-time-symmetric quantum critical phenomena, Nat. Commun. **8**, 15791 (2017).

[17] A. Ghatak and T. Das, Theory of superconductivity with non-Hermitian and parity-time reversal symmetric Cooper pairing symmetry, Phys. Rev. B **97**, 014512 (2018).

[18] L. Pan, S. Chen, and X. Cui, High-order exceptional points in ultracold Bose gases, Phys. Rev. A **99**, 011601(R) (2019); Interacting non-Hermitian ultracold atoms in a harmonic trap: Two-body exact solution and a high-order exceptional point, **99**, 063616 (2019).

[19] Z. Zhou and Z. Yu, Interaction effects on the $\mathcal{PT}$-symmetry-breaking transition in atomic gases, Phys. Rev. A **99**, 043412 (2019).

[20] L. Zhou and X. Cui, Enhanced fermion pairing and superfluidity by an imaginary magnetic field, iScience **14**, 257 (2019).

[21] H. Shackleton and M. S. Scheurer, Protection of parity-time symmetry in topological many-body systems: Non-Hermitian toric code and fracton models, Phys. Rev. Research **2**, 033022 (2020).

[22] R. Hanai and P. B. Littlewood, Critical fluctuations at a many-body exceptional point, Phys. Rev. Research **2**, 033018 (2020).

[23] M. Fruchart, R. Hanai, P. B. Littlewood, and V. Vitelli, Non-reciprocal phase transitions, Nature (London) **592**, 363 (2021).

[24] L. Pan, X. Wang, X. Cui, and S. Chen, Interaction-induced dynamical $\mathcal{PT}$-symmetry breaking in dissipative Fermi-Hubbard models, Phys. Rev. A **102**, 023306 (2020).

[25] J.-S. Pan, W. Yi, and J. Gong, Emergent $\mathcal{PT}$-symmetry breaking of Anderson-Bogoliubov modes in Fermi superfluids, arXiv:2103.00450.

[26] Y.-M. Li, X.-W. Luo, and C. Zhang, $\mathcal{PT}$-symmetry enhanced Berezinskii-Kosterlitz-Thouless superfluidity, arXiv:2107.10391.

[27] D. S. Petrov, Quantum Mechanical Stabilization of a Collapsing Bose-Bose Mixture, Phys. Rev. Lett. **115**, 155302 (2015).

[28] M. Erhard, H. Schmaljohann, J. Kronjäger, K. Bongs, and K. Sengstock, Measurement of a mixed-spin-channel Feshbach resonance in ^{87}Rb, Phys. Rev. A **69**, 032705 (2004).

[29] A. Widera, O. Mandel, M. Greiner, S. Kreim, T. W. Hänsch, and I. Bloch, Entanglement Interferometry for Precision Measurement of Atomic Scattering Properties, Phys. Rev. Lett. **92**, 160406 (2004).

[30] S. Tojo, Y. Taguchi, Y. Masuyama, T. Hayashi, H. Saito, and T. Hirano, Controlling phase separation of binary Bose-Einstein condensates via mixed-spin-channel Feshbach resonance, Phys. Rev. A **82**, 033609 (2010).

[31] A. M. Kaufman, R. P. Anderson, T. M. Hanna, E. Tiesinga, P. S. Julienne, and D. S. Hall, Radio-frequency dressing of multiple Feshbach resonances, Phys. Rev. A **80**, 050701(R) (2009).

[32] C. R. Cabrera, L. Tanzi, J. Sanz, B. Naylor, P. Thomas, P. Cheiney, and L. Tarruell, Quantum liquid droplets in a mixture of Bose-Einstein condensates, Science **359**, 301 (2018).

[33] P. Cheiney, C. R. Cabrera, J. Sanz, B. Naylor, L. Tanzi, and L. Tarruell, Bright Soliton to Quantum Droplet Transition in a Mixture of Bose-Einstein Condensates, Phys. Rev. Lett. **120**, 135301 (2018).

[34] G. Semeghini, G. Ferioli, L. Masi, C. Mazzinghi, L. Wolswijk, F. Minardi, M. Modugno, G. Modugno, M. Inguscio, and M. Fattori, Self-Bound Quantum Droplets of Atomic Mixtures in Free Space, Phys. Rev. Lett. **120**, 235301 (2018).

[35] C. D'Errico, A. Burchianti, M. Prevedelli, L. Salasnich, F. Ancilotto, M. Modugno, F. Minardi, and C. Fort, Observation of quantum droplets in a heteronuclear bosonic mixture, Phys. Rev. Research **1**, 033155 (2019).

[36] Z. Guo, F. Jia, L. Li, Y. Ma, J. M. Hutson, X. Cui, and D. Wang, Lee-Huang-Yang effects in the ultracold mixture of ^{23}Na and ^{87}Rb with attractive interspecies interactions, Phys. Rev. Research **3**, 033247 (2021).

[37] J. Steinhauer, R. Ozeri, N. Katz, and N. Davidson, Excitation Spectrum of a Bose-Einstein Condensate, Phys. Rev. Lett. **88**, 120407 (2002).

[38] S. B. Papp, J. M. Pino, R. J. Wild, S. Ronen, C. E. Wieman, D. S. Jin, and E. A. Cornell, Bragg Spectroscopy of a Strongly Interacting ^{85}Rb Bose-Einstein Condensate, Phys. Rev. Lett. **101**, 135301 (2008).

[39] P. T. Ernst, S. Götze, J. S. Krauser, K. Pyka, D.-S. Lühmann, D. Pfannkuche, and K. Sengstock, Probing superfluids in optical lattices by momentum-resolved Bragg spectroscopy, Nat. Phys. **6**, 56 (2010).

[40] S.-C. Ji, L. Zhang, X.-T. Xu, Z. Wu, Y. Deng, S. Chen, and J.-W. Pan, Softening of Roton and Phonon Modes in a Bose-

Einstein Condensate with Spin-Orbit Coupling, Phys. Rev. Lett. **114**, 105301 (2015).

[41] A. L. Gaunt, T. F. Schmidutz, I. Gotlibovych, R. P. Smith, and Z. Hadzibabic, Bose-Einstein Condensation of Atoms in a Uniform Potential, Phys. Rev. Lett. **110**, 200406 (2013).

[42] I. Gotlibovych, T. F. Schmidutz, A. L. Gaunt, N. Navon, R. P. Smith, and Z. Hadzibabic, Observing properties of an interacting homogeneous Bose-Einstein condensate: Heisenberg-limited momentum spread, interaction energy, and free-expansion dynamics, Phys. Rev. A **89**, 061604(R) (2014).

[43] C. Eigen, A. L. Gaunt, A. Suleymanzade, N. Navon, Z. Hadzibabic, and R. P. Smith, Observation of Weak Collapse in a Bose-Einstein Condensate, Phys. Rev. X **6**, 041058 (2016).

[44] B. Mukherjee, Z. Yan, P. B. Patel, Z. Hadzibabic, T. Yefsah, J. Struck, and M. W. Zwierlein, Homogeneous Atomic Fermi Gases, Phys. Rev. Lett. **118**, 123401 (2017).

[45] K. Hueck, N. Luick, L. Sobirey, J. Siegl, T. Lompe, and H. Moritz, Two-Dimensional Homogeneous Fermi Gases, Phys. Rev. Lett. **120**, 060402 (2018).

[46] L. Zhou, W. Yi, and X. Cui, Dissipation-facilitated molecules in a Fermi gas with non-Hermitian spin-orbit coupling, Phys. Rev. A **102**, 043310 (2020).